A Zenith Delay Model for Precise Kinematic Aircraft Navigation

Oscar L. Colombo, *GEST/NASA Goddard SFC*

BIOGRAPHY

Dr. Oscar L. Colombo works on applications of space geodesy, including gravity field mapping and precise positioning by space techniques, and has been associated with the Space Geodesy group at Goddard for many years. He also develops and test precise very long baseline differential and point-positioning methods with GPS, in cooperation with groups in the USA and abroad.

ABSTRACT

A new mathematical model for estimating and correcting the residual neutral wet and hydrostatic delay of radio waves along aircraft trajectories, calibrated and tested with data from numerical weather models and weather balloons, as well as actual aircraft GPS data, has shown, so far, good promise for its use with or without meteorological information. Further testing, with different kinds of non-GPS "truth" data, is planned for the near future. This model is the sum of four error states, each multiplied by a specially chosen function of height. It represents the residual delay that remains uncorrected, due to imperfections in the refraction correction of GPS data during pre-processing (e.g., with a simple model based on a standard atmosphere). The residual zenith delay estimated with the new model is transformed into slant delay along the path of the radio signals, with the Niell's mapping functions.

The new model is intended for use in precise (sub-decimeter), kinematic, recursive solutions, in very-long-baseline differential and point-positioning navigation, whether carried out in post-processing or in real time.

The recursive, point-positioning, kinematic solutions whose results are shown here, include error states for the rover's position and zenith delay, and for the floated biases of the ionosphere-free linear combination of the L1 and L2 carrier phase (or Lc). In differential mode, the solutions should also include as unknowns the base-stations' residual zenith delays, modeled as simple random walks, one for each fixed site.

The results of the preliminary tests described here, some based on hours of airborne GPS data, suggest that this model is suitable for GNSS kinematic navigation with sub-decimeter precision.

INTRODUCTION

Radio waves propagation in the neutral atmosphere. This paper deals with the correction of the delaying effect of the *neutral atmosphere*—that is, excluding the ionosphere—on the propagation of radio signals of systems such as GPS. Unlike the ionospheric delay, the neutral delay is practically the same at all radio frequencies, so the use of more than one carrier frequency does not help to correct this delay. This neutral delay is usually referred to as "tropospheric refraction' (or "tropo"), although a significant portion of it is due to the air above the tropopause. At any given point P in the atmosphere, the ambient air pressure P, temperature T, and water vapor partial pressure e_w can be use to calculate the *refractivity* $N = 10^6(n-1)$, where n is the refraction index, which is the ratio $n = c/v$ of the speed of light in vacuum c to the phase speed of light v within an infinitesimal volume of air around P. At GPS frequencies, $c > v$, so $n > 1$, and the relationship between N and P, T, and e_w is:

$$N = c_1 P/T + c_2 e_w/T + c_3 e_w/T^2 \qquad (1)$$

c_1, c_2, c_3 are known constants derived from the physical properties of the atmospheric gases. The integral of N with respect to distance along a direct path, or *ray*, followed by radio waves, equals the total neutral delay of those waves as they travel from one end of that ray to the other (e.g., from satellite transmitter to GPS receiver) [1]. This is the basis of the procedure known as *ray tracing* (in actual calculations, N is computed at closely spaced, discrete points along the ray, divided by 10^6, and integrated numerically using, say, Simpson's rule. If the ray is a vertical line drawn between a point P on or above the terrain, and another point directly above it, and at the top of the atmosphere, then the integral of N is the *zenith delay ZD* at P. This delay can be conveniently divided into two components: one that is a function of the total air pressure P at that point (the first term in (1)), known as the *hydrostatic* zenith delay *ZDh*, and a second component that depends only on the partial pressure of water vapor e_w, that is known as the *wet* zenith delay *ZDw* (the sum of the second and third terms in (1)). Also, quite conveniently, the *slant delay SD* along a line from a point

P inside the atmosphere (e.g., the location of a GPS receiver) to another point S outside it (such as the location of a GPS satellite) can be computed as the product of the zenith delay and a *mapping function m*. This is usually given in the form of a continuous fraction, an idea introduced by Marini in 1972 [2], and implemented in various models, including the still widely used Marini-Murray model [3]. The main independent variable is the elevation *E* of the point S above the horizon of P: *m* is approximately equal to the inverse of *sine(E)*. *E* is the "geometric" elevation angle, so the rays are considered to be straight lines between the locations defined by the Cartesian coordinates of P and S, ignoring the effect known as *ray bending*. This effect is important in land surveying, where theodolites, EDM's and similar devices, employ electromagnetic waves often directed near horizontally to a target. For satellite systems, where radar, laser, and other tracking devices are pointed mostly upwards, the problem becomes more tractable. The advent of satellites, and the need to track them precisely, gave added impetus to efforts to calculate better the atmospheric delay along upward pointing rays, resulting in models still widely in use with systems such as GPS. Most models perform quite well down to an elevation between 10 and 20 degrees, below which they become progressively less precise. For very low elevations, extra parameters known as *refraction gradients* have to be added to the models. Since very low elevation signals tend to have poor reception, an elevation cutoff of 10 degrees seems reasonable for kinematic solutions, which are particularly sensitive to poor data. So gradients are not considered here. In some formulations, such as that of Niell [4], [5], *m* can also be given as a function of latitude ϕ, height *H*, and time—in Day Of Year form, as t_{DOY}. In others, such as Herring's [6], the mapping functions are also a function of the ambient temperature *T* at P. There is a wet mapping function m_w, and a hydrostatic function m_h, and they can be used to calculate the total slant delay for a receiver at a given location P as follows:

$$SD_{(total)} = ZD_w\, m_w(E, t_{DOY}, \phi, H) + ZD_h\, m_h(E, t_{DOY}, \phi) \qquad (2)$$

(The independent variables in (2) are those in the Neill mapping functions, which are the ones used in this work.)

MODELLING THE NEUTRAL ATMOSPHERE

Neutral delay models. Many formulas for calculating *SD* as a function of *E* and other variables have been proposed over the years [1, ibid.], calibrated with meteorological data from weather balloons launched at many different places and times of the year, to be used to correct refraction delays. They may or may not be used with local meteorological data measured at P (e.g., *P*, *T*, %humidity *R*, or else e_w derived from *Td*). Some formulas are given in terms of zenith delay and mapping function, as in (2), others are compact, single functions of the same variables. None of the formulas are good enough to correct the satellite data to the extent needed for very precise navigation. So the error in the correction, the *residual troposphere*, has to be estimated by adjusting one or more parameters as part of the navigation solution. The simplest approach is to use nominal values for *P*, *T*, and humidity of an average, or *standard atmosphere*. For example: P = 10015 millibar, $T = 20^oC$, R = 0 (or e_w = 0).
To calculate *ZDw* with meteorological data, the value of the partial water vapor pressure e_w is usually obtained from other quantities, for example temperature *T* and dew point temperature *Td* using the Clausius-Clapeyron equation [7]. In the case of 100% humidity, there can be condensation with or without frost [8]. This affects the value of e_w, but not enough to matter here.

Availability of meteorological data. *P*, *T*, T_d, are quantities that can be measured directly with instruments carried by weather balloons, or that can be obtained from the GRIB-formatted files of numerical weather models (NWM). To understand the effect of the atmosphere on radio signals, in order to develop and validate models of neutral delay, it is essential to have access to that kind of meteorological information.
Fortunately, in recent years a great deal of weather data has been gathered worldwide with satellites, aircraft, weather balloons, GPS receivers, water vapor radiometers, etc., from which global and large-area three-dimensional numerical weather models (NWM) are obtained. These models are constantly updated every few hours. Such NWM models, and much of the meteorological data used to create them, are nowadays openly available over the Internet to scientists, engineers, and also the general public, from NOAA and other organizations. Estimates of water vapor content made with networks of GPS receivers such as GPSMET are also used as data for the NWM [9]. Also in recent years, several studies have been published on the effect of various constituents of the atmosphere on the propagation of radio waves [10]. Propagation delays caused by those parts of the atmosphere visible to the naked eye (mist, clouds, rain drops, snow flakes, ice crystals, hail, dust), have been studied, and found to be, usually, much smaller than the delays due to the invisible components of air: water vapor, nitrogen, oxygen, CO2, and minor quantities of other gases.

Some helpful characteristics of the neutral delay. Figure 1 shows vertical profiles of *T* and T_d, in what is known as a skew T plot (so named because the temperature axis is inclined at 45^o), with total air pressure *P* as the vertical axis variable. This plot has been computed using data from a NWM model, at a geographical location and epoch entered by the user through a graphical interface provided at a Web site run by NOAA, and accessible without restrictions to the general public. In addition, an ASCII data file with this

information in numerical form, repeated at intervals of two hours, can be obtained through the same interface. The irregular, jagged character of these profiles reflects the complexity of the atmosphere.

However, in spite of such complexity, three very helpful facts greatly simplify the modeling of the zenith delay. These facts are:

(1) Both wet and hydrostatic zenith delay components are strongly correlated between points on the same horizontal surface, with correlation lengths of hundreds of kilometers [11].

(2) At any given location, both components usually change very slowly over time, and the residual delay does so at a variable rate of 1-2cm per hour [12], [13].

(3) The vertical profiles of refractivity and, consequently, their integrated values ZD_w and ZD_h, are very smooth functions strongly resembling decaying exponential functions of height above the geoid, or "*sea level*": the *orthometric height H* [14].

Facts (1) and (2) justify the widely used approach of modeling the residual zenith delay with a simple random walk [13, ibid.]. This approach has been used quite successfully with static receivers, in geodesy and meteorology, and in navigation. In the latter case, with receivers on surface vehicles such as ships, cars, trains, etc., the process noise of the random walk may be increased somewhat, to account for the additional change in delay caused by the change in position. But with aircraft, which can change position much more, and much faster, both vertically and horizontally, than other types of vehicle, it is more difficult to find a good dynamic model for that delay, particularly one that is suitable for implementation in a Kalman filter solution [15], [16].

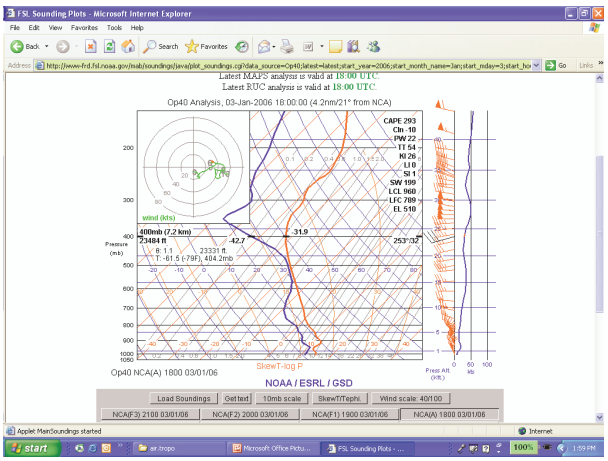

Figure 1. Vertical profiles of temperature (red) and dew point temperature (blue), in a skew T plot at a location specified by the user of this public NOAA Web page. Such plot is created automatically, using information from one of NOAA's Rapid Update Cycle (RUC) NWMs.

With aircraft, the total (wet plus hydrostatic) residual zenith delay is often treated as a random walk with a rather large amount of process noise, or as a white noise, uncorrelated from one (filter update) epoch to the next [16, ibid.].

Taking advantage of some characteristics of the delay. The ideas presented in this paper are inspired on a model developed, at the beginning of this decade, at the University of the Armed Forces, in Munich, by Torben Schueler, as part of the work for his doctoral thesis on combining GPS measurements with pre-existing NWM models [17]. The original use for this model was to condense the very large GRIB-formatted files of the weather models, into much smaller files containing only the information relevant to GPS meteorology, preserving enough information to calculate very precisely the vertical zenith delay profile, and then to convert this delay to total precipitable water vapor content in the column of air on any given location and time within the spatial and temporal coverage of the NWM model. Schueler showed very clearly that, in spite of being shaped by complex physical causes, such vertical profiles can be described quite precisely with a simple expression. In particular, the wet zenith delay can be represented to better than 1 cm, up to heights of more than 10 km, with a decaying exponential function of height, while the hydrostatic zenith delay can be represented, with similar accuracy, with another exponential plus a quadratic function:

$$ZD_w = ZD_{0w}\, exp(-[H-H_0]/Q_w) \pm (< 1cm) \qquad (3a)$$

$$ZD_h = ZD_{0h}\, exp(-[H-H_0]/Q_h) + A\,(H-H_0)^2 + B\,(H-H_0) + C \pm (< 1cm) \qquad (3b)$$

(Notation: "*exp(x)*" means "e^x".) There are seven unknown parameters: 2 *scale factors* ZD_{0w}, ZD_{0h}; 2 positive *scale heights* Q_w, Q_h, and 3 *parabolic terms* A, B, C. H is the orthometric height of P, and H_0 is an orthometric reference height (e.g. sea level (H_0 = 0), the height of a survey marker at an airfield, etc.)

Schueler did not give a second equation for ZD_h; instead, he gave one for the pressure P. But there is a simple relationship between both, so converting from his original formulation to that of (3b) is immediate. The relationship between ZD_h and P, according to Saastamoinen [19], is:

$$ZD_h = 0.0022767\, P / F(\phi, H) \qquad (4a),$$

$$F(\phi,H) = 1-0.00266\cos(2\phi)-0.00028\, H \qquad (4b)$$

P is in millibars (or HPa), and H is in kilometers.

Altogether, there is a total of seven unknown parameters in this model: ZD_{w0}, ZD_{h0}, Q_w, Q_h, A, B, and C. By adjusting them, it is possible to fit very closely the actual zenith delay along the whole column of air. Schueler thoroughly checked the correctness of this 7-parameter model by making extensive use of vertical profiles obtained from global medium-resolution and local high-resolution numerical weather models, and from weather

balloons. I have independently verified that model, and obtained similar results, doing ray-tracing with NOAA's newest high-resolution Rapid Update Cycle, or RUC weather models (13 km grid) covering the mainland of the USA, and its overseas territories. I have done the same thing using weather balloon data, collected in various parts of the world, in different seasons, at heights of between 0 and 20 km. Table 1 shows the results of fitting the exponential part of the 7-parameter model to weather balloon data from different locations in the Northern and Southern hemisphere, during local winter and summer. These are the results of some of the many tests I made with balloon data distributed by NOAA through its unrestricted Web site. The table shows great variability in scale heights, particularly for the wet component, with an excellent exponential fit to the wet component, and a less successful fit to the hydrostatic component, which is why Schueler added three quadratic terms to his model. Because the exponential amplitudes and scale heights in (4a-b) change considerably with horizontal position and with time, these parameters would have to be estimated repeatedly in a kinematic solution for a prolonged, far-ranging survey. In meteorology, for which the model was intended, this is not a problem. But in precise navigation this presents quite a practical challenge, because to estimate those exponential parameters with a linear, Bayesian least squares procedure, would mean using very poor first order approximations to the highly non-linear exponential terms. There are ways to do this, in principle, but it could be quite hard, in practice.

TABLE I
EXPONENTIAL FITS TO ZENITH DELAY PROFILES FROM WEATHER BALLON DATA OF BOREAL WINTER/AUSTRAL SUMMER 2006 (ALL VALUES ARE IN METERS)

SITE NAME Lat, Long (degrees)	SCALE HEIGHT H wet H hydro	RMS OF FIT ZDW MAX |RESIDUAL|	RMS OF FIT ZDH MAX |RESID|
ALASKA (71N, 78W)	3517 6988	0.0007 0.0013	0.015 0.026
S POLE (90S, 00W)	1810 6947	0.0002 0.0003	0.010 0.017
ANTARCTICA (78S, 67E)	1509 7297	0.0003 0.0008	0.008 0.015
CORDOBA (31S, 64W)	1736 8470	0.0089 0.0171	0.018 0.019
BELEM (1S, 38W)	1805 7794	0.0061 0.0133	0.019 0.058
N. ALESUND (79N, 12E)	1160 7361	0.0006 0.0009	0.019 0.050

The goal of my work has been to find a model just as precise and, from the point of view of navigation, simple to program, computationally efficient, and easy to use.

THE NEW MODEL

Finding a linear and compact model. As a first step towards such a model, I found that it was possible to replace, without a significant loss of precision, each of the exponentials in (4a-b) with a linear combination of another two exponentials with scale heights respectively equal to the smallest and to the largest likely values of the scale heights Q_w or Q_h:

$$ZDw = ZD1_w \exp(-[H-H_0]/Q1_w) + ZD2_w \exp(-[H-H_0]/Q2_w) \pm (< 1cm) \quad (5a)$$

$$ZDh) = ZD1h \exp(-[H-H0]/Q1h) + ZD2h \exp(-[H-H0])/Q2h) \pm (< 1cm) \quad (5b)$$

where $Q1_w < Q_w < Q2_w$; $Q1_h < Q_h < Q2_h$.

Replacing in (4a-b) ZD_w and ZD_h according to (5a-b) results in a completely linear model with seven unknown parameters $ZD1_w$, $ZD2_w$, $ZD1_h$, $ZD2_h$, A, B, and C, to be estimated simultaneously with the receiver coordinates and the carrier phase biases in the navigation solution.
Next, I investigated the possibility of reducing the number of parameters without a significant loss of precision. The result was the 4-parameter model defined by the following equations (in bold characters):

$$\mathbf{ZD = ZD1 \exp(-[H-H_0]/Q1_w) + ZD2 \exp(-[H-H_0]/Q2_w) + ZD3 + ZD4 \pm (< 1cm)} \quad (6)$$

The ZD are error states obeying the following first order difference state equations:

$$\mathbf{ZD1(t_i) = ZD1(t_{i-1}) + W1t(t_i) + W1d(t_i) + B1} \quad (7a)$$
$$\mathbf{ZD2(t_i) = ZD2(t_{i-1}) + W2t(t_i) + W2d(t_i) + B2} \quad (7b)$$
$$\mathbf{ZD3(t_i) = ZD3(t_{i-1}) + W3t(t_i) + W3d(t_i) + W3h(t_i) + B3} \quad (7c)$$
$$\mathbf{ZD4(t_i) = W4(t_i)} \quad (7d)$$

The B's are constant biases, and the W's are zero-mean Gaussian white process noise components, with variances:

$$\mathbf{var\{Wj_t\} = (\sigma^2_{jt}) (t_i-(t_{i-1}))} \quad (8a)$$
$$\mathbf{var\{Wj_d\} = (\sigma^2_{jd})(\Delta d(t_i, t_{i-1}))} \quad (8b)$$
$$\mathbf{var\{W3_h\} = (\sigma^2_h)(H(t_i)-H(t_{i-1}))} \quad (8c)$$
$$\mathbf{var\{W4\} = \sigma^2_4} \quad (8d)$$
$$\mathbf{var\{Bk\} = \sigma^2_{Bk}} \quad (8e)$$

Here, j = 1, 2; k = 1,2, 3; t_i, t_{i-1} are any two consecutive epochs when the filter is updated (not necessarily equally spaced); $\Delta d(t_i, t_{i-1})$ is the distance between the rover positions at times t_i and t_{i-1}; $H(t_i)$ is the height of the rover at epoch t_i ; finally, the σ's are the standard deviations of the B's and W's. All W's are 0 at the initial epoch (t_0); so $ZDj(t_0) = Bj$, for j = 1, 2, 3; and $ZD4(t_0) = 0$.

The coefficients (or "partials") of the error states, in the observation equations, are the products of those in (6), multiplied by Niell's wet (*ZD1, Z*D2) and dry (*ZD3*) mapping functions, and by a constant equal to one (*ZD4*). So the corresponding terms in the observation equation for the residual phase or code range $\Delta\rho$ are:

$$\Delta\rho = ZD1\,[m_w(E,\phi,t_{DOY},H)\,\exp(-(H-H_0)/Q1_w)] + ZD2\,[m_w(E,\phi,t_{DOY})\,\exp(-(H-H_0)/Q2_w)] + ZD3\,[m_h(E,\phi,t_{DOY},H) + ZD4 + \ldots \quad (9)$$

Here $\Delta\rho$ is the observed minus the computed range (after applying some standard refraction correction), and "+..." indicates navigation error states not related to refraction.
The new model was tested and tuned both with data simulated along various aircraft trajectories using information from a high-resolution weather model, and with actual GPS aircraft data. As a result, the following values were chosen for the fixed scale heights $Q1_w$, $Q2_w$ in (6) and the σ's in (8a-e):

$$\sigma_{1t} = \sigma_{2t} = \sigma_{3t} = 0.005\ m/(minute)^{1/2} \quad (10a)$$
$$\sigma_{1d} = \sigma_{2d} = \sigma_{3d} = 0.005\ m/(km)^{1/2} \quad (10b)$$
$$\sigma_{3h} = 0.04\ m/(m/200m)^{1/2} \quad (10c)$$
$$\sigma_4 = 0.005\ m \quad (10d)$$
$$\sigma_{B1} = \sigma_{B2} = \sigma_{B3} = 0.1\ m \quad (10e)$$
$$Q1_w = 1000m \quad (10f)$$
$$Q2_w = 3000m \quad (10g)$$

In (10c) "*(m/200m)*" indicates that the height change between filter updates is measured in units of 200m. Therefore, the unknowns to be estimated, or *refraction error states* are three *bias plus random-walk* states: *ZD1*, *ZD2*, *ZD3*, and one *white noise* error state *ZD4*.
From the state equations (7a-d), it follows that the corresponding *state transition matrix* is diagonal, with diagonal elements equal to 1 (for *ZD1*, *ZD2*, *ZD3*), and 0 (for *ZD4*); this simplifies and speeds up calculations in the filter (and the smoother), because matrix/vector and matrix/matrix products become the trivial operations: "do nothing about the elements related to *ZD1*, *ZD2*, *ZD3*", and "set the elements related to *ZD4* to 0". (The complete state vector in a precise kinematic solution has many more components, besides the four states of the refraction model: receiver coordinates, carrier phase Lc biases, etc.)
According to (7a-d), each of the four states of the model is driven by some combination of three types of process noise, with variances proportional to the change in vehicle height, distance, and in time elapsed between consecutive filter updates. The first two states correspond to the wet zenith delay, and the third to the hydrostatic component; the three, combined, represent the residual zenith delay at airplane altitude: the actual zenith delay minus a zenith delay correction made to the data during pre-processing. The fourth state could represent the error in a hydrostatic correction based on air pressure measurements, calculated with equation (4a-b). In this study, it has been used to monitor the misclosure of the model: the smaller the absolute value of *ZD4*, the better the sum of the other three terms may cancel out the residual refraction, as intended. Reassuringly, the absolute value of *ZD4* never exceeded 0.0001m in any of the tests carried out.
By setting to 0 some of the process noise and biases uncertainties, effectively "shutting off" part of the model, it is possible to end up with either the white noise or random-walk models often used in precise GPS navigation. Different procedures used for this kind of navigation tend to give different results, particularly in height, as shown in a recent comparison of airplane trajectories calculated with different kinematic software, and the same data (from low-altitude flights across the North Atlantic) [19]. This could be due, primarily, to differences in the treatment of refraction.
The ideas underlying the present model also can be used to develop and validate future models, for new applications, such as measuring the precipitable water vapor with GPS receivers carried on a variety of vehicles, in places such as oceans, where the more usual observations of pressure, temperature, and humidity may be too difficult, expensive, or impossible to make.

TESTING THE MODEL

Approach. For testing, I implemented the new delay model in "IT", a program for geodetic surveying and precise navigation, which runs under Windows (Win98 and later), UNIX, LINUX, System X, and FreeBSD, that I continue to develop, and to share, with a Free Software Foundation General License, with collaborators.
I made two kinds of test: (a) with simulated data derived from a high-resolution NWM; (b) with actual GPS data. I made (a) first, for a preliminary validation of the model, and for an initial calibration of its bias and process noise variances. Those tests consisted of Kalman filter solutions to estimate zenith delays from data simulated with a variety of flight trajectories and meteorological conditions, to find the minimum number of states, with the right amount of *a priori* uncertainty, so that the post-fit residuals would be consistently small, and the zenith delay recovered, never more than a few millimeters off the "true" (simulated) values. Once this initial stage seemed successfully accomplished, I began tests with real GPS data. Originally I had expected to carry out tests with additional, non-GPS "truth" (or control) data, to verify the results even better. Unfortunately, those flights could not take place as expected this year, so the results presented here are not the final ones. So a different kind of test had to be made. Simulated zenith delays were added to the GPS data. The idea was that, if the model is good, adding an artificial, but realistic, atmospheric signal should cause only minor changes in the kinematic solution, because the added signal would be largely removed by the filter, along with the actual delay. However, the sum of the realistic signal and the actual delay cannot be much larger than a

normal delay. The Kalman filter is likely to be "stressed" by unrealistically large delays, since the *a priori* values of the bias and process noise uncertainties (the sigmas in 10a-e), calibrated for normal delays, may prove too small to estimate correctly much larger delays.

The GPS flight data. To test the model as fully as possible, the kinematic solutions were made in Precise Point Positioning (PPP) mode, so the results would be more sensitive to the effect of the atmosphere than in differential mode, with no cancellation of the slant delays at the rover with those at reference sites.
Of the GPS data available, the most adequate were from a flight in Svalbard (Spitzbergen), in the Arctic, in July of 2005. The data were collected by members of Professor Tevi Murray's group, now at Swansea University, in Wales, as part of a project to map glaciers with an airborne laser altimeter.
In addition to the 10Hz dual-frequency data from the GPS receiver on the airplane, the research team collected, simultaneously, similar data from several land receivers, including a very distant one, KELY, in Kangerlussuaq, on the West coast of Greenland. The reason for getting the Greenland data was to compare two long baseline, differential, kinematic software, by "navigating" with each one of them a fixed site with very well known (cm-level) coordinates that could be used as "truth", after correcting for the earth-tide. The test was arranged by Matt King, at the University of Newcastle upon Tyne. The KELY site is one of the permanent IGS stations. This offers two special advantages: (1) a time-series of precise estimates of the actual zenith delay for the day of the flight is available from the Analysis Center at the Geodaetisches Forschung Zentrum (GFZ), in Potsdam; (2) being one of the IGS Reference Frame Stations (RFS), a 30-second subset of the 1Hz GPS data was probably used to calculate the precise orbits and 30-second clocks for that day at the CODE center in Berne, later made available through the CDDIS data archive at NASA Goddard Space Flight Center. Those orbits and clocks should have errors whose negative effect on the PPP solution may be smaller than otherwise, because they share some of the data, so they are less likely to obscure the effect of the delay model being tested.
A similar case is the Svalbard flight, as the airplane was always relatively near NYAL, the IGS RFS site at Ny-Alesund. The airplane took off and landed back on the same airfield, near Longyearbyen, flew some 80km to a glacier, and then proceeded to traverse over it, at a height of about 1400 meters, collecting altimeter data (Figs. 6 and 7). The flight lasted some 2hours and 15 minutes. The airfield is 58m above sea level.

Simulating the neutral delay. To obtain the artificial, but realistic, delays needed for validating and calibrating the model, I made use of digital maps of *ZDw* on the terrain, and of air pressure reduced to mean sea level ("altimeter"), produced with real meteorological data by NOAA for its Northeast HA-NDGPS Test in 2004, and distributed freely over the Internet (Figure 2). I converted the air pressure to ZD_{h0} with (4a-b), and chose H_0 = 230 (the height at KELI, i.e. ignoring the shape of the topography in the case of ZD_w).
I interpolated linearly each zenith delay, first in space, along the straight line between the two nearest grid points on the map, to the instantaneous horizontal position of the imaginary aircraft, and then in time, between the values at that position obtained from consecutive maps (the pair of maps in Fig. 2 is one of a series of "snapshots" taken at two-hour intervals), and finally upper continued those results to the airplane altitude H using Schueler formulas (3a-b), with wet and hydrostatic scale heights Q_w = 2500m, and Q_h = 7500m, respectively. H was the height along an imaginary flight path, with the ground track shown with a thin horizontal blue line in the ZD_w map of Figure 2 (left), and a vertical flight profile consisting of a an initial climb at a fixed rate of 200m/min, to a predetermined height, followed by a period cruising at that height, always with the same ground speed, and ending with a final descent, at the same vertical rate as during the climb, but with opposite sign, all the way down to the starting altitude.

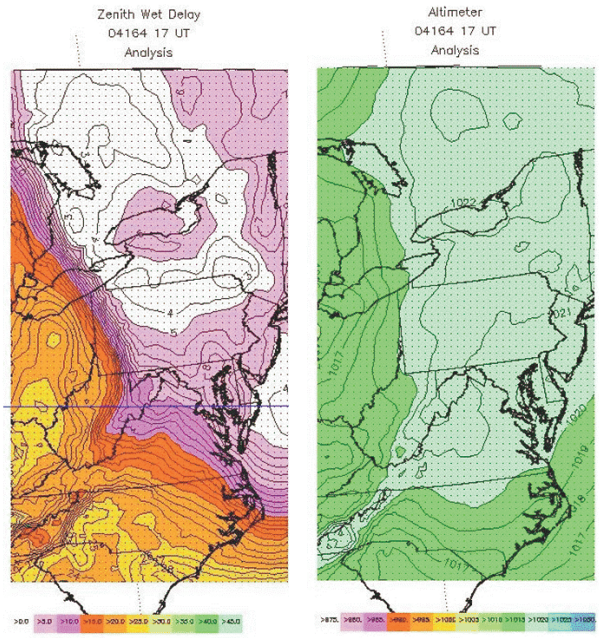

Figure 2. Zenith wet delay (left), and pressure reduced to mean sea-level ("altimeter", right). Blue line shows simulated flight ground track (850km long). 30cm of ZD_w near the start (at the line's leftmost point), only to 4cm at the end. The plane flies over places where air moisture is high, and also where the air is dry. (Grid points are dark dots regularly arranged in rows and columns.)

To calibrate the model, I computed the zenith delay along a number of such simulated flights, all with the same

duration, epoch, and ground track, but each with a different ground speed and altitude profile.

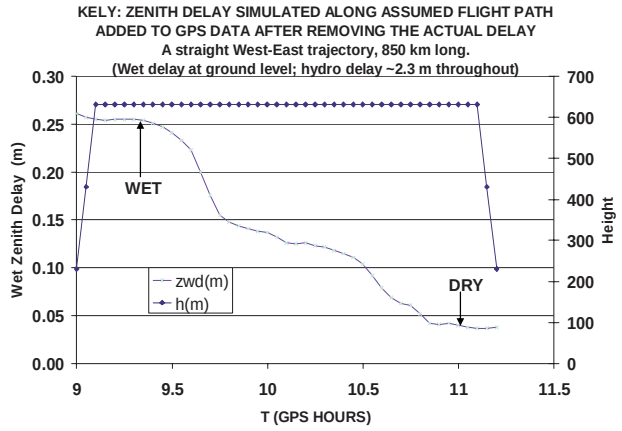

Figure 3. The simulated wet zenith delay (light blue), plotted along the blue line of Fig. 2, and the vertical flight profile (dark blue) used in the test with the Svalbard aircraft data. Zd_h was ~2.3m (not shown here).

Tests with GPS data. Two such tests were made: one with data from Greenland, the other from the airplane's receiver, in Svalbard. For each, a simulated *ZD* was calculated assuming a ground-speed of 120m/s, so the full 850km "ground track" was "flown" in about 2hs, 15min.

(1) The Greenland Test. The 1Hz data provided by the operators of the IGS site KELY was post-processed using the PPP method, to obtain a kinematic trajectory of estimated instantaneous positions. These were compared to the known, fixed position of the site, after correcting for the earth tide. The site position being known with sub-cm precision, the vertical (Up), East (E), and North (N) discrepancies between instantaneous and known coordinates are, in fact, the errors in the kinematic solution, except for a small constant 3-D offset, which is the error in the site coordinates. Those discrepancies are plotted in Figure 4, along with their global statistics: their mean vector (or 3-D) offset, their 3-D RMS about the mean, and their largest 3-D vector modulus. Those values are typical of a precise, post-processed, PPP solution, with good orbits and good 30-second clocks.

The solution was repeated with the data modified as follows: the precisely estimated total zenith delay computed at GFZ, and obtained in ASCII format from the CDDIS archive at Goddard, was converted to slant delay in the direction of each satellite, with the Niell "dry" mapping function. The excess range corresponding to this delay was subtracted from the data. The simulated total zenith delay, calculated along an imaginary flight line with the vertical profile shown in Figure 3, and converted to slant delay with the same Niell mapping function, was then added to the data, virtually replacing the real delay with the simulated one. The solution was then repeated. The discrepancies between this new solution and the known coordinates of KELY are shown in Figure 5. Comparing the plots for the new solution to those of Fig. 4 one can see very little change (1-2cm) in the global statistics, and a noticeable, but small change in the shape of the plots. This is at it should be, if the new refraction model is working well, helping eliminate most of the delay regardless of whether it is the true one or the simulated one, so the very small residual delay left uncorrected cannot affect either solution significantly.

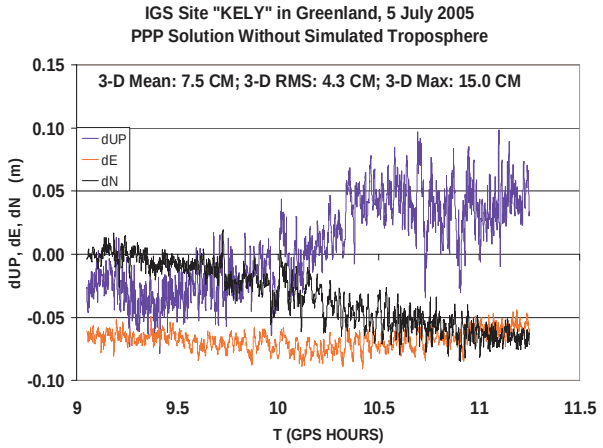

Figure 4. The discrepancies between the instantaneous position of KELY, according to the PPP kinematic solution, and the published precise coordinates of this IGS site. Solution made with the unmodified GPS data. 3-D Mean: 7.5cm, 3-D RMS: 4.3cm, 3-D Max.: 15cm. Up (blue), East (red), North (black).

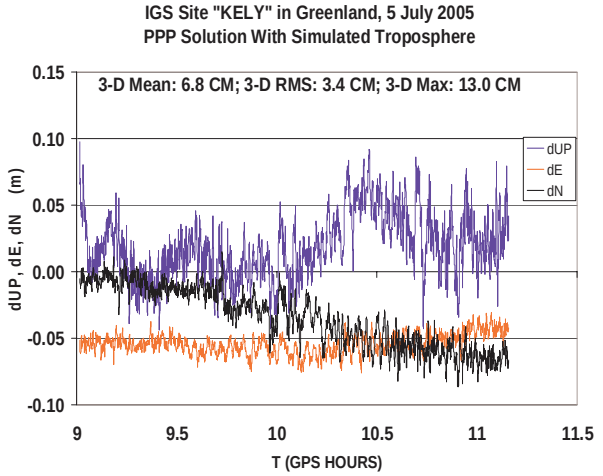

Figure 5. Same as Fig. 4, but with the true delay, based on the actual total *ZD* (as estimated at the IGS Analysis Center GFZ, in Potsdam), replaced with a simulated delay calculated along the flight path defined by the blue line ("ground track") in Fig. 2, using meteorological data from the NOAA's NE Test, and the vertical profile shown in Fig. 3. 3-D Mean: 6.8cm, 3-D RMS: 3.4cm, 3-D Max.: 13cm. These values are very similar to those in Fig. 3.

(2) The Svalbard airplane test. Figure 6 shows the actual ground track of the airplane during a flight in Svalbard. The plane took off from the Longyearbyen airfield, and flew to survey a glacier some 80km to the NW, where it followed a series of traverses during the actual survey, mapping the ice surface with a laser altimeter. Then it returned and landed on the same airfield. Figure 7 shows the actual height profile of the same flight, and the simulated zenith delay at the altitude of the airplane (based on the meteorological data shown in Fig. 2), upper-continued from mean sea level with the Schueler equations (4a-b). The exponential decay of the main terms of those equations explains the "inverted" shape of the delay plot: both components of refraction decrease, as the airplane ascends and there is less air and water vapor left above it. (There is virtually no water vapor at heights above 5km).

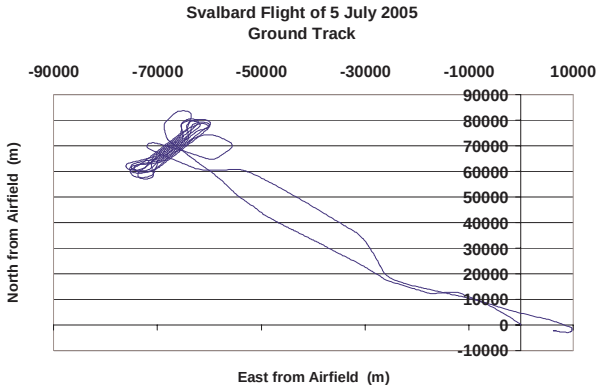

Figure 6. The ground track of the Svalbard flight.

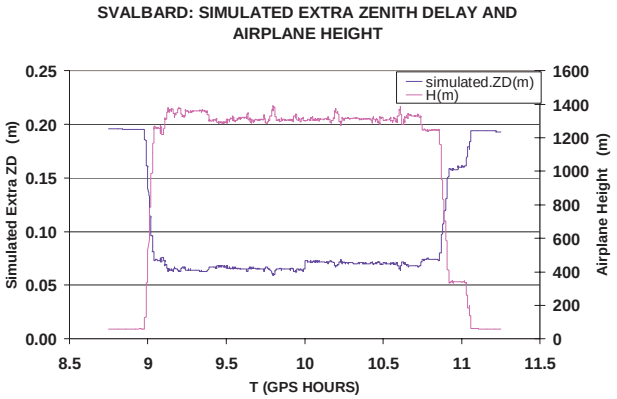

Figure 7. The height profile of the Svalbard flight (magenta), and the simulated total *ZD* (minus a nominal *ZD*) at aircraft height (blue).

Since, unlike KELY, there is no precise, independent estimate of the zenith delay for the airplane, a nominal zenith delay $ZD_{nom} = 2.27exp(-0.000116\ H)$ [m] was subtracted from the simulated zenith delay, to avoid ending up with a modified delay twice as large as normal, which could have "stressed" the filter.

The Niell hydrostatic mapping function was used, as in the KELY test, to convert *ZD* to slant delay *SD*. Figure 8 shows the difference between two PPP solutions made with and without the artificial delay added to the GPS data. Because of problems with the data during the first five minutes of the session, the takeoff and the first half of the climb are missing in both precise PPP kinematic solutions. The difference between the two solutions is an indication of how useful the new model could be for mitigating the effect of the neutral delay on the solution. The global statistics are shown also in the Figure. It is encouraging to see that the largest difference is 6.7cm.

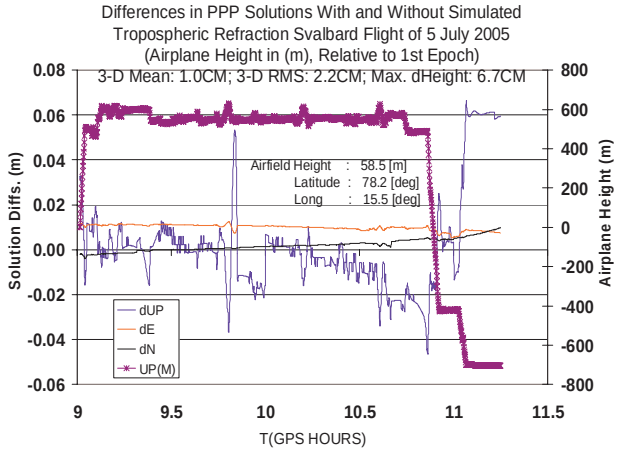

Figure 8. Differences between the PPP kinematic solution of the Svalbard flight with and without adding the extra delay corresponding to the simulated *ZD* shown in Fig. 7. 3-D Mean: 1cm, 3-D RMS: 2.2cm, Max. Discrepancy: 6.7cm

CONCLUDING REMARKS

The tests conducted so far indicate that the new refraction model could be used for aircraft navigation of sub-decimeter precision, at heights ranging from sea level to 20km. It is computationally efficient and easy to implement within a recursive trajectory determination scheme, be it in real-time or in post-processing, in precise differential or point-positioning modes.

The mathematical delay model is completely linear in its four error states. It subsumes the widely used single-state white noise and random walk models, since it can be reduced to either by setting to zero some of the state initial values, *a priori* variances, and process noise components.

The model needs to be tested and tuned further, with more simulations and with more real satellite data, under a wider variety of conditions. The results should be verified with strong "truth" data. I expect that such additional tests will take place in the near future.

ACKNOWLEDGEMENTS

My thanks to Torbe Schueler, at the Universitaet der Bundeswehr, in Munich, for providing me with some of his global TROPEX files, which helped me greatly to understand the variability of the wet and hydrostatic scale heights worldwide, with location and season; to Tavi Murray and the SLICES team, for the GPS data, and a pleasant visit with them in Swansea; to Matt King, in Newcastle, for arranging the software intercomparison that started me thinking again about the need for a better refraction model; to Marcelo Santos, at UNB, for keeping me up to date on related research there; to Jim Ray (NOAA), for alerting potential users like me, to the availability of the Northeast HA-NDGPS Test data, and where to find other information; to Seth Gutman (NOAA), for publishing the data of the Northeast Test on the Internet, and helping me understand the GPSMET network. Finally, a big "thank you" to all the dedicated people at NOAA and other organizations who have made research such as this possible by posting a great deal of meteorological data, relevant literature, and other useful information on the Internet, so anybody with a PC and a broadband connection can access and use it.

REFERENCES

[1] Spilker, J.J., Tropospheric Effects on GPS, in "*Global Positioning System: Theory and Applications*", Bradford, B.W., Spilker, J.J, Axelrad, P., and P. Enge (eds), Vol I, Ch. 13, AIAA series "*Progress in Aeronautics and Astronautics*", Vol. 163, Washington, D.C. 1996.

[2] Marini, J.W., Correction of Satellite Tracking Data for an Arbitrary Tropospheric Profile, *Radio Science*, Volume 7, Number 2, pp. pp. 223-231, February 1972

[3] Marini, J.W., and C. W. Murray, Correction of Laser Range Tracking Data for Atmospheric Refraction at Elevations above 10 Degrees, NASA report X-591-73-351, Goddard Space Flight Center, 1973.

[4] Niell, A.E., Global Mapping Functions for the Atmosphere Delay at Radio Wavelengths, J. Geophys. Res., Vol. 101, pp. 3227-3246, 1996.

[5] Niell, A.E., Improved atmospheric mapping functions for VLBI and GPS, *Earth, Planets, Space*, 52, pp. 699-702, 2000.

[6] Herring, T. A., Modeling Atmospheric Delays in the Analysis of Space Geodetic Data, in: De Munk, J. C and T.A. Spoelstra (eds.), in *Refraction of Trans-atmospheric Signals in Geodesy*, N.G.C., Publ. on Geodesy, New Series, Number 36, The Hague, The Netherlands, May 1992

[7] Hanssen, R., *Atmospheric Heterogeneities in ERS Tandem SAR Interferometry,Chapter 2*, pp. 8-24, DEOS Report No. 98.1, Delft University Press, 1998.

[8] Honeywell , Honeywell Hvac - Moisture Tutorial, in: *http://content.honeywell.com/building/components/Hycal_Html/moist.asp*, 1999.

[9] Gutman, S.I., Sahm, S.R., Benjamin,S.G., Schwartz, B.E., Holub, K.L., Stewart, J.Q., and T.L. Smith, Rapid Retrieval and Assimilation of Ground Based GPS Precipitable Water Observations at the NOAA Forecast Systems Laboratory: Impact on Weather Forecasts. J. Met. Soc. Japan, 82(1B), pp. 351-360, 2004.

[10] Solheim, F.S., Vivekanandan, J., Ware, R.H., C. Rocken, Propagation Delays Induced in GPS Signals by dry Air, Water Vapor, Hydrometeors, and other Particulates, . Geophys. Res., Vol. 104, No. D8, pp. 9663–9670, April 27, 1999

[11] Elgered, G., Sensing the Temporal and Spatial Distribution of Atmospheric Water Vapor Using GPS, Presentation by Gunnar Elgered, Onsala Space Observatory, Chalmers University of Technology, kge@oso.chalmers.se

[12] Elgered, G., et. al., Observing Moving Air Masses with a GPS Network, Geophysical Research Letters, vol.24, pp.2663-2666, 1997.

[13] Herring, T.H., Davis, J.L., I.I. Shapiro, Geodesy by Radio Interferometry:The Application of Kalman Filtering to the Analysis of Very Long Baseline Interferometry Data, J. of Geophys. Res., Vol. 95, No. B8, pp. 12,561-12,581, August 10, 1990.

[14] Nievinski, F., Covel, K., Santos, M., Wells, D., R. Kingdon, Range-Extended GPS Kinematic Positioning using Numerical Weather Prediction Model, Proceedings ION Annual Technical Meeting, Boston, pp. 27-29 June, 2005.

[15] Collins, P., Langley, R.B., J. LaMance, Limiting Factors in Tropospheric Propagation Delay Error Modelling for GPS, Airborne Navigation, Proceedings ION 52nd Annual Meeting, Cambridge, Mass., 19th - 21st June, 1996.

[16] Collins, J.P., R.B. Langley, Estimating the Residual Tropospheric Delay for Airborne Differential GPS Positioning (A Summary), Proc. Scientific Assembly of the IAG, Rio de Janeiro, Brazil, September 3-9, 1997.

[17] Schueler, T., On Ground-Based GPS Tropospheric Delay Estimation, PhD Thesis, Universitaet der Bundeswher, Munich, 2001.

[18] Saastamoinen, Atmospheric Correction for the Troposphere and Stratosphere in Radio Ranging of Satellites, in: *The Use of Artificial Satellites for Geodesy*, Henriksen, editor, Geophys. Monogr. Ser., vol. 15, pp. 247-251, AGU, Washington, D.C., 1972

[19] Zhang, X., R. Forsberg, Assessment of Long-range Kinematic GPS Positioning Errors by Comparison with Airborne Laser Altimetry and Satellite Altimetry, J. of Geophysics, in print, 2006.